

See discussions, stats, and author profiles for this publication at: <https://www.researchgate.net/publication/282705576>

# Speed control of BLDC motor by using PID control and self-tuning fuzzy PID controller

**Conference Paper** · September 2014

DOI: 10.1109/REM.2014.6920443

CITATIONS

15

READS

2,278

**2 authors:**



**Mohamed Shamseldin**

Future University in Egypt

**13** PUBLICATIONS **37** CITATIONS

[SEE PROFILE](#)



**Adel A El-Samahy**

Helwan University

**28** PUBLICATIONS **211** CITATIONS

[SEE PROFILE](#)

**Some of the authors of this publication are also working on these related projects:**



Concentrated Solar power [View project](#)



improve the single neuron PID control using different techniques [View project](#)

# *Speed Control of BLDC Motor By Using PID Control and Self-tuning Fuzzy PID Controller*

Mohammed Abdelbar Shamseldin  
Mechatronics Engineering Department  
Future University in Egypt  
Cairo, Egypt  
eng.moh.abd88@gmail.com

Adel A. EL-Samahy  
Electrical Power and Machines Department  
Helwan University  
Cairo, Egypt  
el\_samahya@yahoo.com

**Abstract**— This paper presents three different robust controller techniques for high performance brushless DC (BLDC) motor. The purpose is to test the ability of each control technique to force the rotor to follow a preselected speed/position track. This objective should be achieved regardless the parameter variations, and external disturbances. The first technique is conventional PID controller. The second controller technique use genetic algorithm to adjust the PID controller parameters based on three different cost functions. Finally a self-tuning fuzzy PID controller is developed and tested. These controllers are tested for both speed regulation and speed tracking. Results shows that the proposed self-tuning fuzzy PID controller has better performance.

**Keywords**—PID control; Self-tuning fuzzy PID control; Genetic algorithm;

## I. INTRODUCTION

The development of high performance motor drives is very important in industrial as well as other purpose applications such as steel rolling mills, electric trains, electric automotive, aviation and robotics [1]. Several types of electric motors have been proposed for these types of applications [2]. Among these types, conventional DC motors which are known with their excellent characteristics. On other hand conventional DC motor, have some disadvantages such as routine maintenance of commutators, frequent periodic replacement of brushes and high initial cost [3]. Conventional DC motors cannot be used in clean or explosive environment. Squirrel cage induction motor is alternative to the conventional DC motor. It offers the robustness with low cost. However, its disadvantages have poor starting torque and low power factor [4]. In addition, neither conventional DC motors nor induction motors can be used for high-speed application. The alternative to both conventional DC motor and induction motor is the DC brushless motor, which can be considered the most dominant electric motor for these applications [4]. They are driven by dc voltage but current commutation is done by solid-state switches. The commutation instants are determined by the rotor position and the position of rotor is detected by position sensors or by sensorless techniques [4].

The state space model of BLDC motor is discussed in [4]. This model derived for BLDC motor in arbitrarily reference frame. One of the major drawbacks of such a model is the dependency of the state variables coefficients on the rotor position (time dependent), which make difficult to implement

[5]. This problem may be alleviated by considering the model presented in [5] and adopted in this paper. The coefficients of state variables using this model are constant with time. This is the main advantage of such a model.

In high performance drives applications such as robotics, dynamic actuation and guided manipulation, moving the end effector from one position to other is not the only objective, the end effector while traveling must follow a pre-selected time tagged trajectory at all times [1]. This must be achieved even when the system loads, inertia, and parameters are varying, to achieve this objective the control strategy must be adaptive, robust, accurate and simple to implement [1-4]. The PID controller is applied in various fields in engineering owing to its simplicity, robustness, reliability and easy tuning parameters [1]. The famous method to find PID parameters *Ziegler-Nichols* rule but sometimes are not the best. So, it can be realized by using genetic optimization technique based on three different cost functions to find the best PID control parameters. The main obstacles facing PID control technique is sudden change in set point and parameter variation, it makes the PID control gives poor response [4]. This problem can be alleviated by implementing advanced control techniques such as adaptive control, variable structure control, fuzzy control and neural network. One of the major problems with implementation of self-tuning adaptive control techniques is inability to achieve the trajectory control in the presence of sudden disturbances or large noises. This is because the parameter estimator might provide erroneous results in the presence of sudden disturbances or large noises [6]. Variable structure controller is simple but it difficult to implement. This is because of the possibility of the abrupt change in the control signal, which might affect the system operation [2]. A neural-network-based motor control system has a strong ability to solve the structure uncertainty and the disturbance of the system, whereas it requires more computing capacity and data storage space [4]. Fuzzy control theory usually provides non-linear controllers that are capable of performing different complex non-linear control action even for uncertain non-linear systems [1]. Unlike conventional control designing, a FLC does not require precise knowledge of the system model such as the poles and zeroes of the system transfer function [1]. A fuzzy-logic control system based on expert knowledge database needs less calculations, but it lacks sufficient capacity for the new rules [4]. So, the combination between fuzzy and PID controller for tuning the PID parameters according to the error and change of error might be a good alternative. It is

simple, robust, and adaptive. This combination is called self-tuning fuzzy PID controller which will be compared with the best PID controller which has been verified by genetic algorithm technique at different disturbances.

## II. MATHEMATICAL MODEL OF BLDC MOTOR

### A. Transfer function model

The transfer function is one of the most important concepts of control theory, and the transfer-function-based mathematical models are widely used in automatic control fields. Some control design and analysis methods, such as the root-locus method and the frequency-response method, are also developed based on the system transfer function.

Suppose that the three-phase BLDC motor is controlled by the full-bridge driving in the two-phase conduction mode [4].

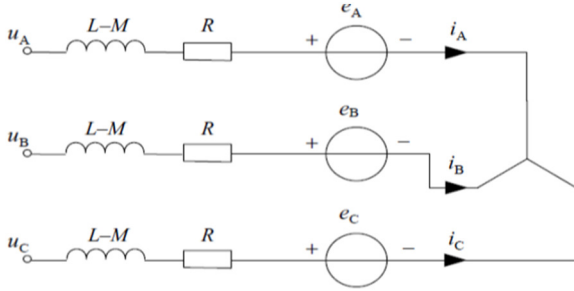


Fig. 1. Equivalent circuit of the BLDC motor

The mechanisms of back-EMF and electromagnetic torque are all the same with those of the traditional brushed DC motor, thus similar analysis methods can be adopted.

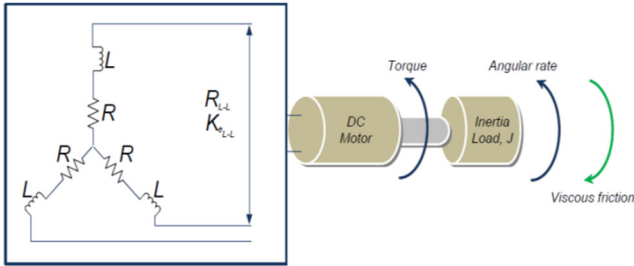


Fig. 2. Brushless DC Motor Schematic Diagram

At any time the two phases are excited either AB or BC or CA. the simplified equivalent circuit will be as Fig. 3.

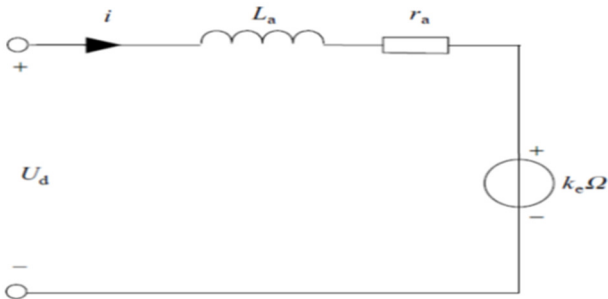


Fig. 3. Simplified equivalent circuit of the BLDC motor

$$i_A = -i_B = i \quad (1)$$

$$\frac{di_A}{dt} = -\frac{di_B}{dt} = \frac{di}{dt} \quad (2)$$

$$u_{AB} = 2Ri + 2(L - M)\frac{di}{dt} + (e_A - e_B) \quad (3)$$

$$\because e_B = -e_A \quad (4)$$

$$\begin{aligned} u_{AB} &= U_d = 2Ri + 2(L - M)\frac{di}{dt} + 2e_A \\ &= r_a i + L_a \frac{di}{dt} + K_e \Omega \end{aligned} \quad (5)$$

$$K_T i - T_L = J \frac{d\Omega}{dt} + B_v \Omega \quad (6)$$

Assume Torque load  $T_L = 0$ .

$$i = \frac{J}{K_T} \frac{d\Omega}{dt} + \frac{B_v}{K_T} \Omega \quad (7)$$

Substitute (7) in (5)

$$U_d = r_a \left( \frac{J}{K_T} \frac{d\Omega}{dt} + \frac{B_v}{K_T} \Omega \right) + L_a \frac{d}{dt} \left( \frac{J}{K_T} \frac{d\Omega}{dt} + \frac{B_v}{K_T} \Omega \right) + K_e \Omega$$

$$U_d = \frac{L_a J}{K_T} \frac{d^2 \Omega}{dt^2} + \frac{r_a J + L_a B_v}{K_T} \frac{d\Omega}{dt} + \frac{r_a B_v + K_e K_T}{K_T} \Omega \quad (8)$$

Using Laplace transform

$$G_u(S) = \frac{\Omega(S)}{U_d(S)} = \frac{K_T}{L_a J S^2 + (r_a J + L_a B_v)S + (r_a B_v + K_e K_T)} \quad (9)$$

By the same method

$$G_L(S) = \frac{\Omega(S)}{T_L(S)} = -\frac{r_a + L_a S}{L_a J S^2 + (r_a J + L_a B_v)S + (r_a B_v + K_e K_T)} \quad (10)$$

The speed response of BLDC motor affected together by applied voltage and load torque.

$$\begin{aligned} \Omega(S) &= G_u(S)U_d(S) + G_L(S)T_L(S) \\ &= \frac{K_T U_d(S)}{L_a J S^2 + (r_a J + L_a B_v)S + (r_a B_v + K_e K_T)} - \\ &\quad \frac{r_a + L_a S}{L_a J S^2 + (r_a J + L_a B_v)S + (r_a B_v + K_e K_T)} \end{aligned} \quad (11)$$

Where:

$U_d$ : DC bus voltage.

$e_A$ : Phase back emf.

$r_a$ : Line resistance of winding,  $r_a = 2R$ .

$L_a$ : Equivalent line inductance of winding,  $L_a = 2(L - M)$ .

$J$ : Rotor moment of inertia.

$T_L$ : Load torque,  $i$ : line current.

$\Omega$ : Rotor speed.

$B_v$ : Viscous friction coefficient.

$K_e$ : Coefficient of line back-EMF.

$K_T$ : Coefficient of line torque constant.

$M$ : Mutual linkage, assume  $M = 0$ .

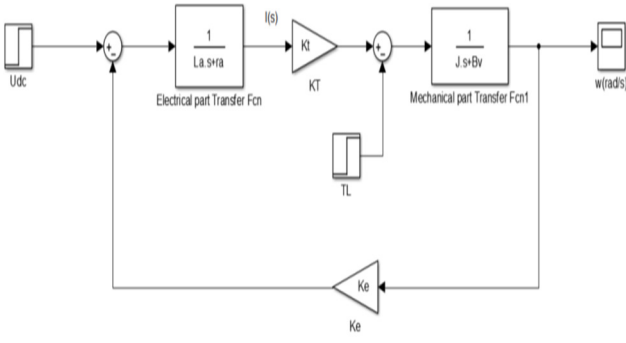


Fig. 4. Structure of BLDC motor transfer function on Matlab Simulink

Fig. 4 shows Structure of BLDC motor transfer function on Matlab Simulink.

### B. State-space model

State-space equation method is one of the most important analysis method in modern control theory. The state-space method is becoming more and more popular in designing control systems with the fast development of computer techniques [4].

$$i_A + i_B + i_C = 0 \quad (12)$$

$$u_{AB} = r_a(i_A - i_B) + L_a \frac{d}{dt}(i_A - i_B) + e_{AB} \quad (13)$$

$$u_{BC} = r_a(i_A + 2i_B) + L_a \frac{d}{dt}(i_A + 2i_B) + e_{BC} \quad (14)$$

Subtract equation (13) from equation (14)

$$u_{AB} - u_{BC} = -3r_a - 3L_a \frac{d}{dt}i_B + e_{AB} - e_{BC} \quad (15)$$

$$\dot{i}_B = -\frac{r_a}{L_a}i_B - \frac{1}{3L_a}(u_{AB} - e_{AB}) + \frac{1}{3L_a}(u_{BC} - e_{BC}) \quad (16)$$

By the same method.

$$u_{AB} = r_a(2i_A + i_B) + L_a \frac{d}{dt}(2i_A + i_B) + e_{AB} \quad (17)$$

$$u_{CA} = r_a(i_C - i_A) + L_a \frac{d}{dt}(i_C - i_A) + e_{CA} \quad (18)$$

Subtract equation (17) from equation (18).

$$(u_{AB} - e_{AB}) - (u_{CA} - e_{CA}) = 3r_a i_A + 3L_a \frac{d}{dt}i_A \quad (19)$$

$$\dot{i}_A = -\frac{r_a}{L_a}i_A + \frac{1}{3L_a}(u_{AB} - e_{AB}) - \frac{1}{3L_a}(u_{CA} - e_{CA}) \quad (20)$$

$$u_{AB} = u_{BC} \quad (21)$$

$$e_{AB} = e_{BC} \quad (22)$$

$$u_{CA} = -(u_{AB} + u_{BC}) = -2u_{AB} \quad (23)$$

$$e_{CA} = -(e_{AB} + e_{BC}) = -2e_{AB} \quad (24)$$

By substitute (21), (22), (23), (24) in (20) will become.

$$\dot{i}_A = -\frac{r_a}{L_a}i_A + \frac{1}{3L_a}(u_{BC} - e_{BC}) + \frac{2}{3L_a}(u_{AB} - e_{AB}) \quad (25)$$

From equation (6).

$$\dot{\Omega} = \frac{-B_v}{J}\Omega + \frac{1}{J}(T_e - T_L) \quad (26)$$

Where

$$T_e = K_T i \quad (27)$$

$$\begin{bmatrix} \dot{i}_A \\ \dot{i}_B \\ \dot{\Omega} \\ \dot{\Theta} \end{bmatrix} = \begin{bmatrix} -\frac{r_a}{L_a} & 0 & 0 & 0 \\ 0 & -\frac{r_a}{L_a} & 0 & 0 \\ 0 & 0 & \frac{-B_v}{J} & 0 \\ 0 & 0 & 1 & 0 \end{bmatrix} \begin{bmatrix} i_A \\ i_B \\ \Omega \\ \Theta \end{bmatrix} + \begin{bmatrix} \frac{2}{3L_a} & \frac{2}{3L_a} & 0 \\ \frac{-1}{3L_a} & \frac{1}{3L_a} & 0 \\ 0 & 0 & \frac{1}{J} \\ 0 & 0 & 0 \end{bmatrix} \begin{bmatrix} u_{AB} - e_{AB} \\ u_{BC} - e_{BC} \\ T_e - T_L \end{bmatrix} \quad (28)$$

Where  $\Theta$  is rotor position.

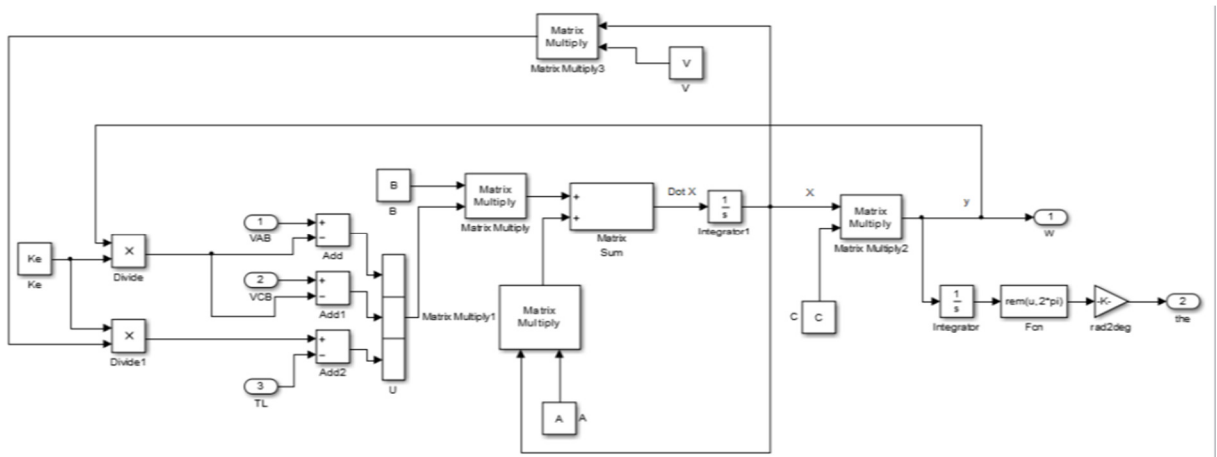


Fig. 5. Structure of BLDC motor state-space model on matlab

Fig. 5 shows the structure of BLDC motor state-space model on matlab Simulink.

### C. Open loop response of BLDC motor

The validity of the models (T.F & S.S) verified by comparing the simulation results of these models with matlab model. The results show that the response of the presented models are identical. The parameters of BLDC motor will show in the following table I.

TABLE I. BLDC motor parameters per phase.

Rating	Symbol	Value	Units
DC resistance	R	0.25	$\Omega$
Inductance	L	0.32	mH
Maximum Flux linkage	$\psi_m$	65	mV/rad/sec
Number of Poles	p	8	
Peak torque	$T_p$	2.83	NM
Rated Voltage	V	15	V
Rotor Inertia	J	0.0042	Kg.m <sup>2</sup>
Friction coefficient	$B_v$	0.0096	N.M.S
Power	P	472	W
Rated current	I	43.5	A

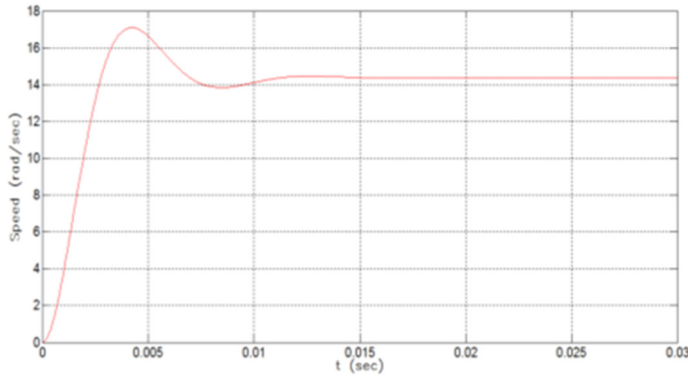


Fig. 6. Open loop speed response without load

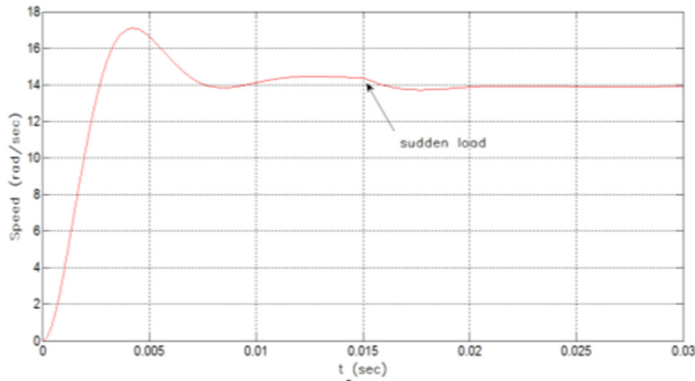


Fig. 7. Open loop speed response with load

Fig. 6 shows the open loop response of motor free running and Fig. 7 shows the speed response with applying sudden load of 30% of full load at t=0.015 sec.

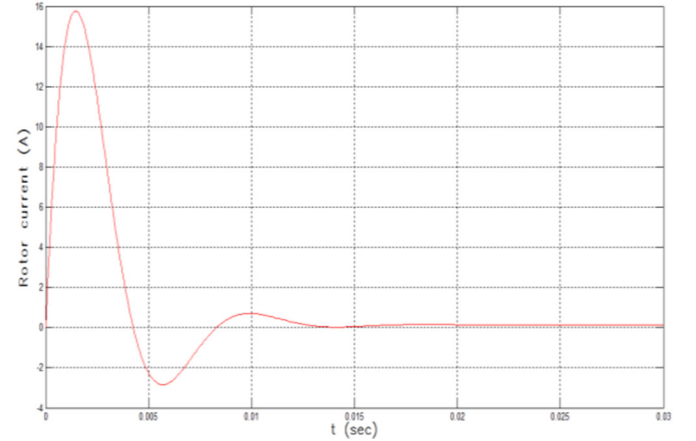


Fig. 8. Rotor current response without load

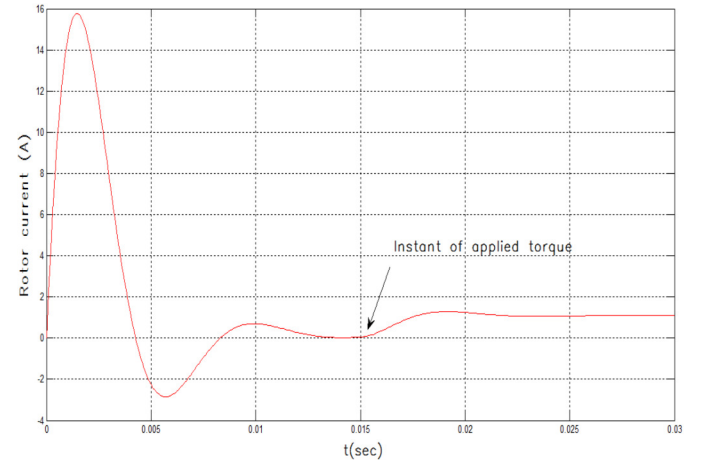


Fig. 9. Rotor current response with load

Fig. 8 shows the starting current is very high and decrease to reach almost zero at no load. Fig. 9 shows the Rotor current of motor free running and applying sudden load of 30% of full load at instant 0.015 sec the current will increase from zero A to 1 A while the speed drops from 14.3 rad/s to 13.8 rad/s.

## III. SPEED CONTROL

### A. PID control

The transfer function of the PID controller is  $K(s) = K_p + \frac{K_i}{s} + K_d s$ . Where  $K_p$ ,  $K_i$ ,  $K_d$  are proportional, integral and differential gains respectively. The function of each part of a PID controller can be described as follows, the proportional part reduces the error responses of the system to disturbances, the integral part eliminates the steady-state error, and finally the derivative part dampens the dynamic response and improves the system stability [8]. The problem in the PID controller is to choose the three parameters to be suitable for the controlled plant. There are many methods to define the parameters of PID controller such as try and error and Ziegler-Nichols methods but most of these methods are rough roads. In this, paper the parameters of PID controllers obtained by Ziegler-Nichols

methods and three different cost function genetic algorithm techniques.

### 1) First cost function

This cost function as shown in (29) minimizes the integrated square error  $e(t)$ .

$$f_1 = \int_0^\infty (e(t))^2 dt \quad (29)$$

### 2) Second cost function

The actual closed-loop specification of the system with controller, rise time ( $t_r$ ), maximum overshoot ( $M_p$ ), settling time ( $t_s$ ), and steady state error ( $e_{ss}$ ) are used to evaluate the cost function. This is done by summing the errors between actual and specified specification as given by (30).

$$f_2 = \frac{1}{[c_1(t_r - t_{rd}) + c_2(M_p - M_{pd}) + c_3(t_s - t_{sd}) + c_4(e_{ss} - e_{ssd})]} \quad (30)$$

Where,  $c_1 : c_4$  are positive constants (weighting factors), their values are chosen according to prioritizing their importance, ( $t_{rd}$ ) is the desired rise time, ( $M_{pd}$ ) is the desired maximum overshoot, ( $t_{sd}$ ) is the desired settling time, and ( $e_{ssd}$ ) is the desired steady state error.

### 3) Third cost function

A performance criterion in the time domain is proposed as given in (31).

$$f_3 = \frac{1}{(1 - e^{-\beta})(M_p + e_{ss}) + e^{-\beta}(t_s - t_r)} \quad (31)$$

This cost function can satisfy the designer requirement using the weighting factor value ( $\beta$ ). The factor is set larger than 0.7 to reduce over shoot and steady-state error [7]. If this factor is set smaller than 0.7 the rise time and settling time will be reduce. All of these cost functions have been minimized subjected to:

$$K_{P \min} \leq K_P \leq K_{P \max}$$

$$K_{i \min} \leq K_i \leq K_{i \max}$$

$$K_{d \min} \leq K_d \leq K_{d \max}$$

The following table summarizes the values the PID parameters obtained from Z.N. and the three cost functions.

TABLE II. Values of PID gains

Controller method	$K_P$	$K_i$	$K_d$
Z.N. method	0.135211	135.211	3.38e-5
First cost function	0.0661	133.9689	0
Second cost function	0.084	104.105	0
Third cost function	0.112	146.698	0

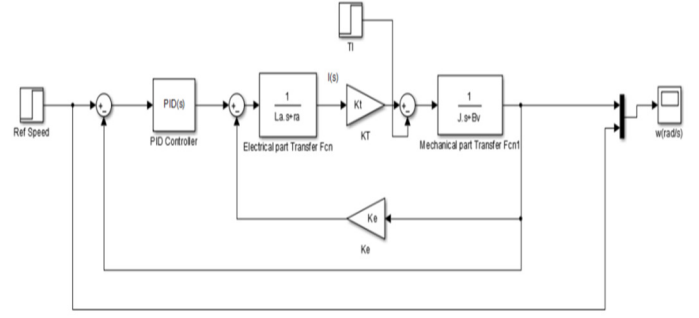


Fig. 10. Structure of BLDC PID speed control by Simulink matlab

Fig. 10 shows the simulink block diagram of the closed loop system using PID controller.

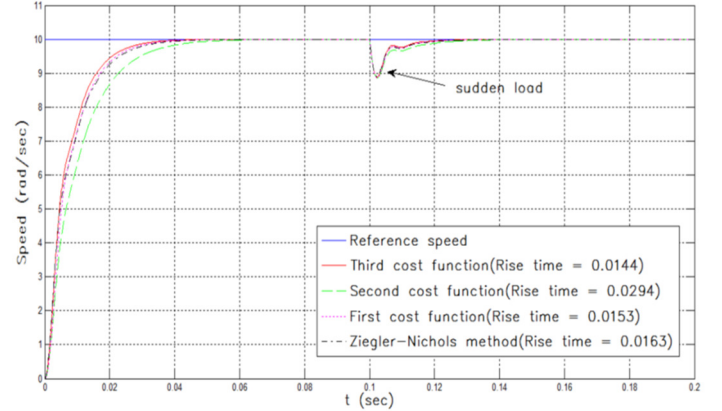


Fig. 11. Comparison between Z-N PID and three-cost function genetic optimization

Fig. 11 shows that the performance of the third-cost function controller has the best performance among the controller techniques.

### B. Self-tuning fuzzy PID controller

Tuning the parameters of a PID controller is very important in PID control. Ziegler and Nichols proposed the well-known method to tune the coefficients of a PID Controller and improve the performance by optimization the PID parameters using different optimization techniques but cannot guarantee to be always effective [8]. For this reason, this paper investigates the design of self-tuning for a PID controller. The controller includes two parts: conventional PID controller and fuzzy logic control (FLC) part, which has self-tuning. Capabilities to track different set point. The proportional, integral and derivate ( $K_p$ ,  $K_i$  and  $K_d$ ) are the gains of PID controller which, tuned on-line to force the system to follow the specified reference (point/track) [5].

Now the control action of the PID controller after self-tuning can be describing as:

$$U^{PID} = K_{p2}e(t) + K_{i2} \int e(t) + K_{d2} \frac{de(t)}{dt}$$

As shown in fig. 12.

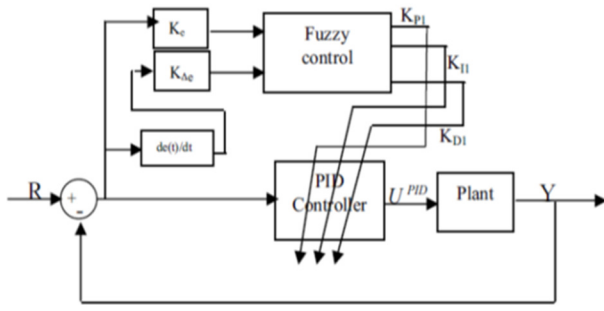


Fig. 12. Structure of self-tuning PID fuzzy controller

Where  $K_{p2}$ ,  $K_{i2}$  and  $K_{d2}$  are the new gains of PID controller and are equals to:

$$K_{p2} = K_{p1} * K_p, K_{i2} = K_{i1} * K_i \text{ and } K_{d2} = K_{d1} * K_d.$$

Where  $K_{p1}$ ,  $K_{i1}$  and  $K_{d1}$  are the gains output of fuzzy control, that are varying online with the output of the system under control and  $K_p$ ,  $K_i$  and  $K_d$  are the initial values of the conventional PID control. The general structure of fuzzy logic control is represented in fig.13 and comprises three principal components.

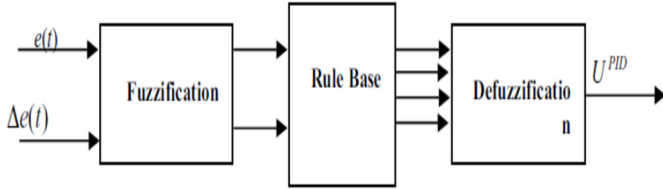


Fig. 13. Fuzzy logic control structure

#### 1) Fuzzification

This converts input data into suitable linguistic values. As shown in fig. 13. There are two inputs to the controller: error and rate change of the error signals. For the system under study the universe of discourse for both  $e(t)$  and  $\Delta e(t)$  may be normalized from  $[-1,1]$ , and the linguistic labels are {Negative Big, Negative, medium, Negative small, Zero, Positive small, Positive medium, Positive Big} and are referred to in the rules bases as {NB,NM,NS,ZE,PS,PM,PB}, and the linguistic labels of the outputs are {Zero, Medium small, Small, Medium, Big, Medium big, very big} and referred to in the rules bases as {Z,MS, S, M, B, MB, VB}. Figure 14&15 shows the memberships of inputs and output of fuzzy logic control.

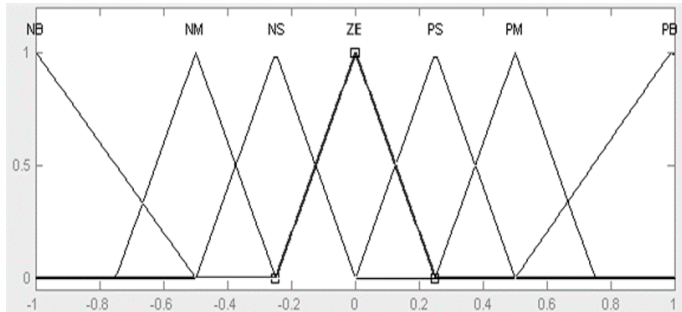


Fig. 14. Memberships function of inputs (e, Δe)

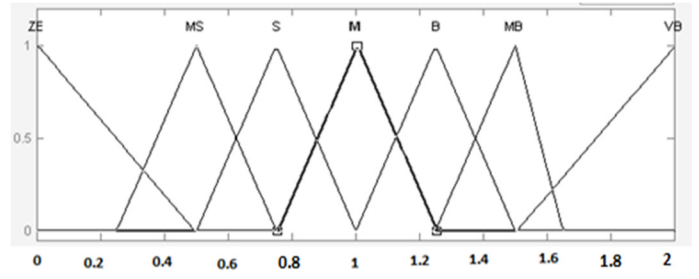


Fig. 15. Memberships functions of outputs ( $K_{p1}$ ,  $K_{i1}$  and  $K_{d1}$ )

#### 2) Rule base

A decision making logic which is, simulating a human decision process, inters fuzzy control action from the knowledge of the control rules and linguistic variable definitions. The rule base is simplified in tables III, IV and V. The input  $e$  has 7 linguistic labels and  $\Delta e$  has 7 linguistic labels. Then we have  $7 \times 7 = 49$  rule base. In this paper simplify 49 to 25 rule base [9].

TABLE III. The Rule base of  $K_{p1}$

$\Delta e/e$	NB	NS	ZE	PS	PB
NB	VB	VB	VB	VB	VB
NS	B	B	B	MB	VB
ZE	ZE	ZE	MS	S	S
PS	B	B	B	MB	VB
PB	VB	VB	VB	VB	VB

TABLE IV. The Rule base of  $K_{i1}$

$\Delta e/e$	NB	NS	ZE	PS	PB
NB	M	M	M	M	M
NS	S	S	S	S	S
ZE	MS	MS	ZE	MS	MS
PS	S	S	S	S	S
PB	M	M	M	M	M

TABLE V. The Rule base of  $K_{d1}$

$\Delta e/e$	NB	NS	ZE	PS	PB
NB	ZE	S	M	MB	VB
NS	S	B	MB	VB	VB
ZE	M	MB	MB	VB	VB
PS	B	VB	VB	VB	VB
PB	VB	VB	VB	VB	VB

#### 3) Defuzzification

This yields a non fuzzy control action from inferred fuzzy control action. The most popular method, center of gravity or center of area is used for defuzzification.



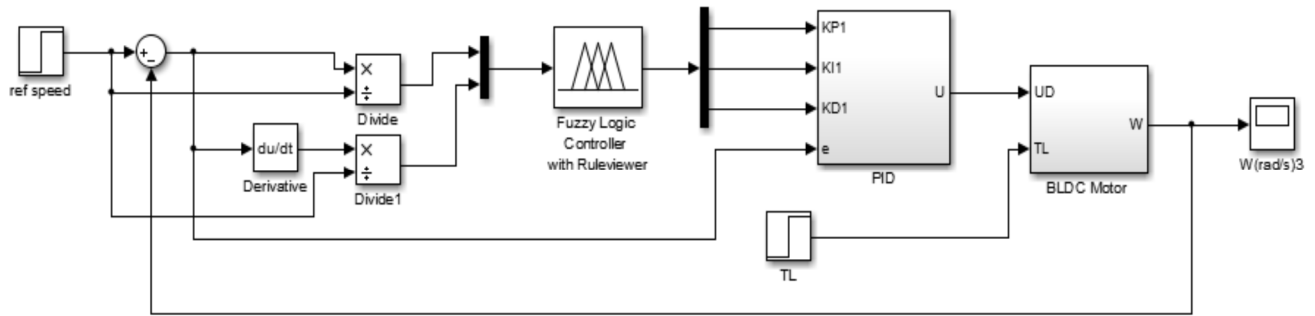


Fig. 16. Structure of self-tuning fuzzy PID controller by Simulink

Fig. 16 shows the structure of self-tuning fuzzy PID controller by matlab Simulink. The controller of self-tuning fuzzy PID controller consists of two parts PID controller and fuzzy logic controller, which tuned on-line the PID controller gains.

#### IV. THE SPEED RESPONSE OF PID CONTROLLER AND SELF-TUNING FUZZY PID CONTROLLER AT DIFFERENT DISTURBANCES

##### A. Speed regulation at sudden load

Fig. 17 shows that the self-tuning fuzzy PID controller is faster response than PID controller with acceptable overshoot and has the ability to track the reference speed in less time than PID controller at sudden load of 70% of full load.

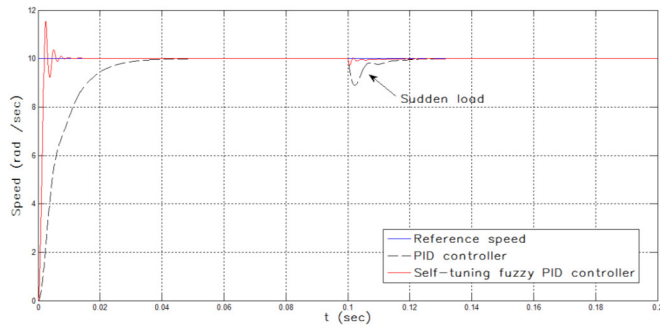


Fig. 17. PID control and self-tuning fuzzy PID controller response at sudden load

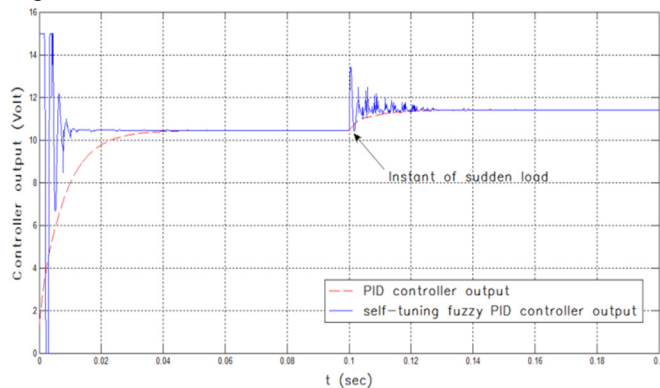


Fig. 18. PID control and self-tuning fuzzy PID controller output at sudden load

Fig. 18 shows the both of controller output the PID controller and the self-tuning fuzzy PID controller.

##### B. Parameter variation

Resistance change of BLDC motor. By decreasing the resistance to 50% and apply sudden load of 70% of full load. You may note in fig. 19 the ability of self-tuning fuzzy PID controller that accommodates the disturbance in a short time.

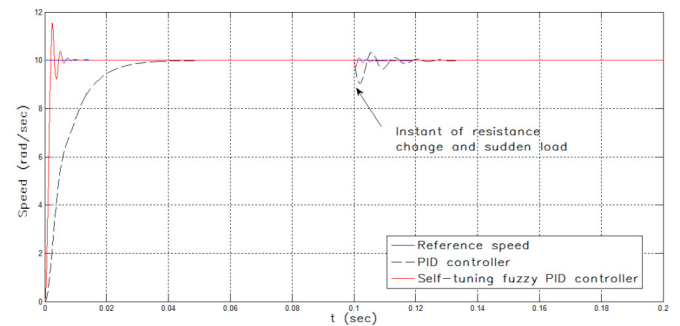


Fig. 19. PID controller and self-tuning fuzzy PID controller response at resistance change and sudden load

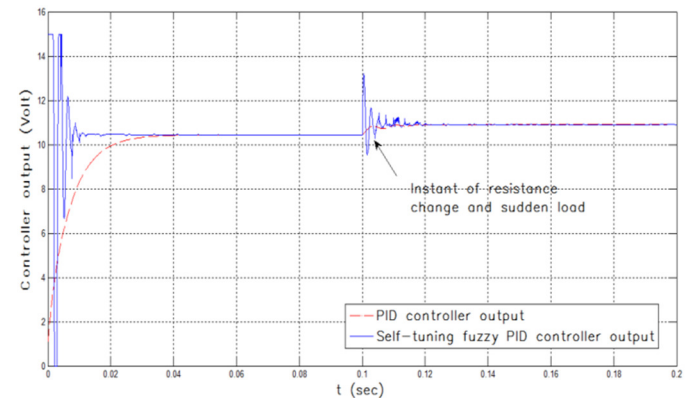


Fig 20. PID controller and self-tuning fuzzy PID controller output at resistance change and sudden load

Fig. 20 shows the PID controller and the self-tuning fuzzy PID controller output at resistance change and sudden load.



### C. Speed regulation at sinusoidal load

Most of applications of robotics exposed to sinusoidal load because of movement of links of robot so need robust control to regulate the speed of BLDC motor. Applying sinusoidal load on BLDC motor as in fig. 21.

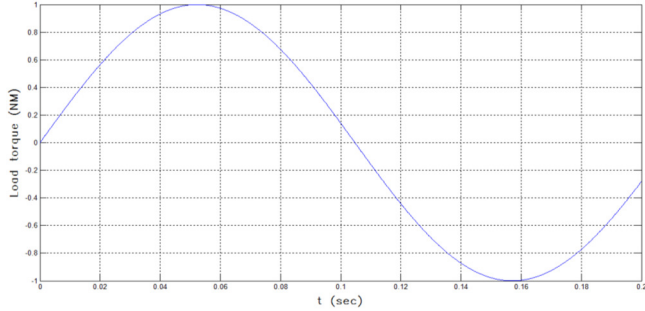


Fig. 21. Sinusoidal load torque that exposed to the BLDC motor during simulation

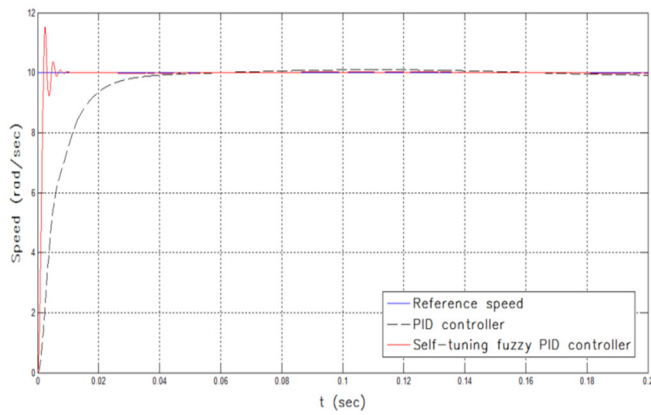


Fig. 22. PID controller and self-tuning PID fuzzy controller response at sinusoidal load

Fig. 22 shows that the self-tuning fuzzy PID controller has faster response and has a little steady state error comparing with the PID controller.

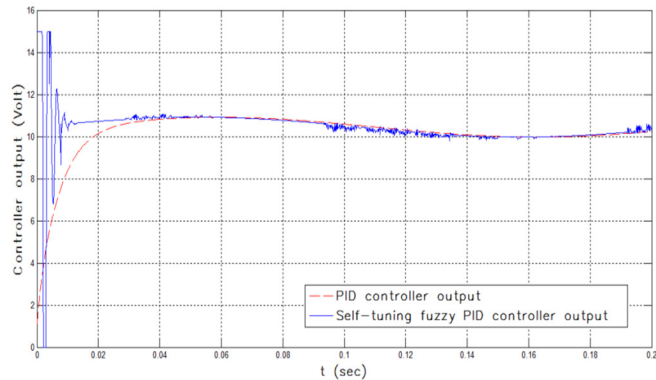


Fig. 23. PID controller and self-tuning PID fuzzy controller output at sinusoidal load

Fig. 23 shows the PID controller and the self-tuning PID fuzzy controller output at sinusoidal load.

### D. Speed tracking

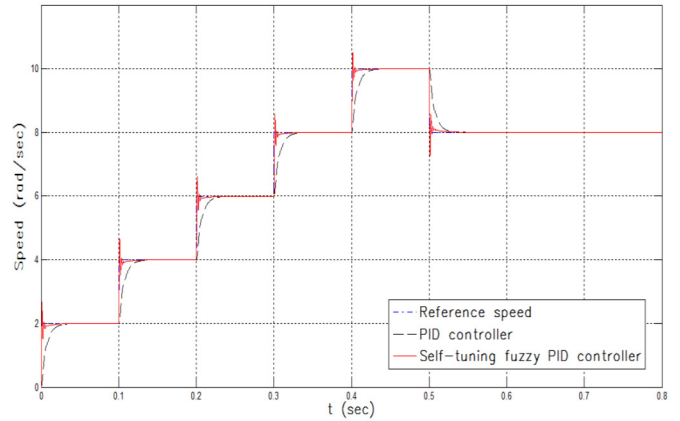


Fig. 24. PID controller and self-tuning PID fuzzy controller response at speed tracking

Fig. 24 shows that the self-tuning fuzzy PID controller is faster than PID control for speed tracking and almost identical on the reference speed.

## V. CONCLUSION

In this paper a three different control techniques are implemented in order to achieve a good speed regulation/tracking regardless the presence of external disturbances and/or parameter variations. The first technique is the famous PID controller. The second controller technique use genetic algorithm to adjust the values of the controller parameters by minimizing three different cost functions. The third technique is the fuzzy PID in which the controller parameters are not constant and continuously adaptively updated according to the error and the change error in order to achieve the required speed tracking. Results shows that the proposed fuzzy PID has better performance compared to the other two techniques.

## REFERENCES

- [1] J. Zhang, N. Wang and S. Wang, "A developed method of tuning PID controllers with fuzzy rules for integrating process," Proceedings of the American Control Conference, Boston, 2004, pp. 1109-1114.
- [2] M. A. EL-Sharkawi, "Development an Implementation of High Performance Variable Structure Tracking Control for Brushless Motors," IEEE Transaction on Energy Conversion, Vol. 6, no. 1 March 1991, pp. 114-119.
- [3] W. R. Pearson and Paresh C. Sen, "Brushless DC Motor Propulsion Using Synchronous Motor for Transient System," IEEE Transection on Industrial Electronics, Vol. IE 31, No. 4, Nov. 1984, pp. 326-351.
- [4] C.-L. Xia, Permanent Magnet Brushless DC Motor Drives and Controls. Singapore: John Wiley & Sons Singapore Pte. Ltd., 2012.
- [5] M. Thesis, "BLDC Motor Modelling and Control – A Matlab ®/Simulink ® Implementation –," 2005.
- [6] Ming Liang Chen "Multi-Layer Self Tuning Powe System Stabilizer," Ph. D. Thesis, University of Washington, 1989.
- [7] A. Mohamed, "Optimization Techniques for Tuning the Controller of a Permanent Magnet Brushless Motor," Cairo, master of science, 2012.
- [8] H.X.Li and S.K.Tso, "Quantitative design and analysis of Fuzzy Proportional-Integral- Derivative Control- a Step Towards Autotuning", International journal of system science, Vol.31, No.5, 2000, pp.545-553.
- [9] G.R.Chen and T.T.Pham, "Introduction to fuzzy sets, fuzzy logic, fuzzy control system", CRC.Press,Boac Raton,FL,USA,2000.

- [10] I. Science, "PID Parameters Optimization by Using Genetic Algorithm Andri Mirzal, Shinichiro Yoshii, Masashi Furukawa."
- [11] M. Omar, M. Soliman, A. M. A. Ghany, and F. Bendary, "Optimal Tuning of PID Controllers for Hydrothermal Load Frequency Control Using Ant Colony Optimization," vol. 5, no. 3, pp. 348–360, 2013.
- [12] J. P. Anderson, A. Julian, F. Approved, and O. M. B. No, "NAVAL POSTGRADUATE AND CONTROL OF A 4th ORDER ROTATIONAL by," no. December, 2009.
- [13] R. Kandiban and R. Arulmozhiyal, "Speed Control of BLDC Motor Using Adaptive Fuzzy PID Controller," *Procedia Eng.*, vol. 38, pp. 306–313, Jan. 2012.
- [14] N. Tadriss, H. Zeroug, and B. Boukais, "Development of brushless d.c. motor drive system for teaching purposes using various PWM control techniques," *Int. J. Electr. Eng. Educ.*, vol. 49, no. 3, pp. 210–231, Jul. 2012.
- [15] P. Agarwal and A. Bose, "Brushless Dc Motor Speed Control Using Proportional-Integral And Fuzzy Controller," vol. 5, no. 5, pp. 68–78, 2013.
- [16] O. J. Oguntuyinbo, "PID CONTROL OF BRUSHLESS DC MOTOR AND ROBOT TRAJECTORY PLANNING AND SIMULATION WITH," 2009.